

## Supporting Information

for *Adv. Sci.*, DOI 10.1002/adv.202300881

ANO1-Mediated Inhibition of Cancer Ferroptosis Confers Immunotherapeutic Resistance through Recruiting Cancer-Associated Fibroblasts

*Fangli Jiang, Keren Jia, Yang Chen, Congcong Ji, Xiaoyi Chong, Zhongwu Li, Feilong Zhao, Yuezong Bai, Sai Ge, Jing Gao, Xiaotian Zhang, Jian Li\*, Lin Shen\* and Cheng Zhang\**

## Supporting Figures and Supporting Tables

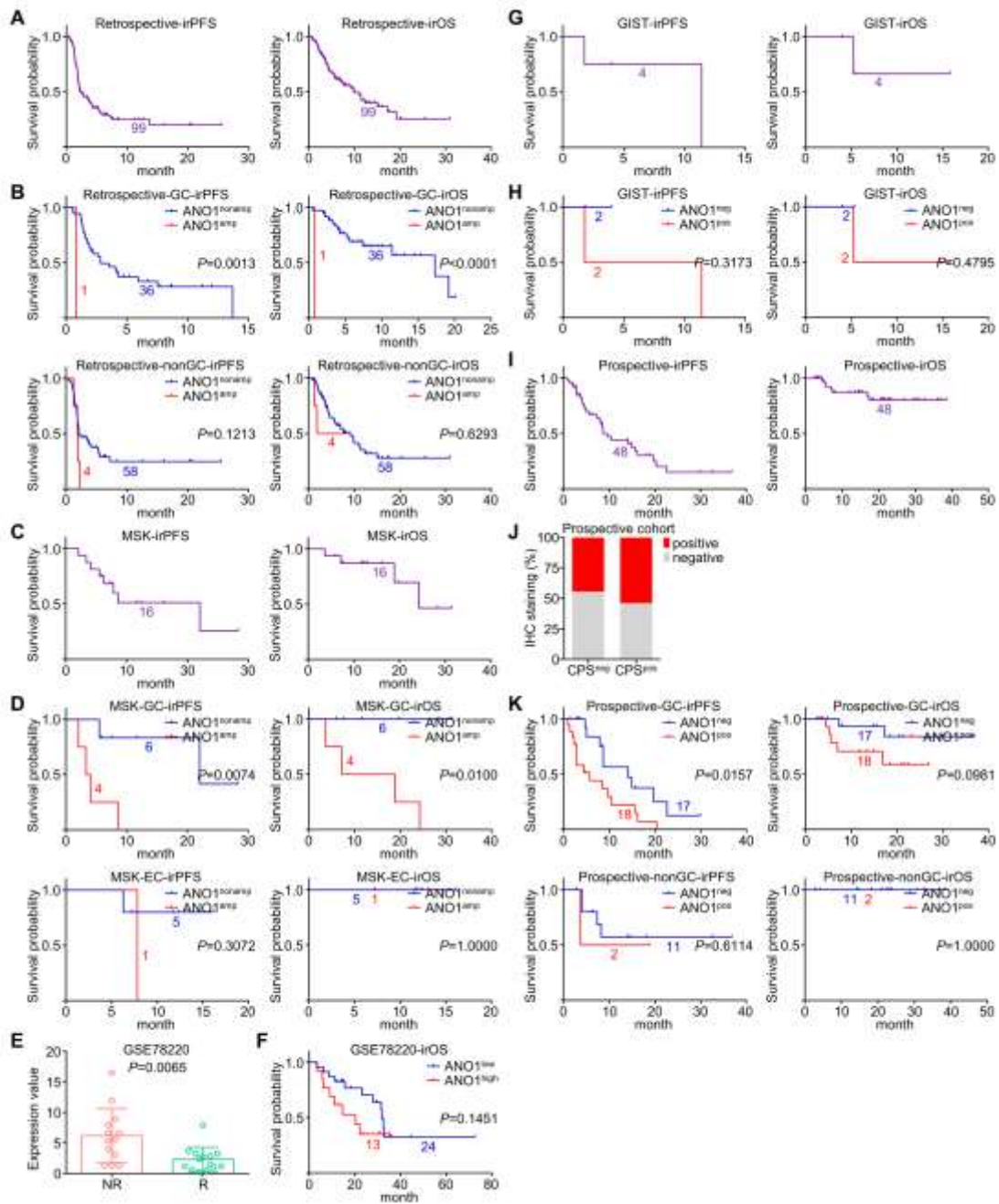


**Figure S1. Further stratification for ANO1's indication to immunotherapeutic outcomes.**

(A) Overall irPFS/irOS for the 99-case GI cancer retrospective cohort received immunotherapy. (B) The prognostic correlation of ANO1 amplification in training cohort was measured for patients of GC and EC+CRC+other cancers. (C) Overall irPFS/irOS for the MSK dataset. (D) The prognostic correlation of ANO1 amplification in MSK dataset was measured for patients of GC and EC. (E) The immunotherapeutic responses and (F) irOS for melanoma GSE78220 cohort were stratified by ANO1 expression. (G) Overall irPFS/irOS for four GIST patients received immunotherapy. (H) irPFS/irOS for GIST patients were stratified by IHC-based ANO1-positivity. (I) Overall irPFS/irOS for the 48-case GI cancer prospective cohort received immunotherapy. (J) Comparison of IHC-based ANO1 positivity between CPS-negative (CPS=0) and -positive (CPS≥1) patients in the prospective cohort. (K) The

prognostic correlation of ANO1-positivity in the prospective cohort was measured for patients of GC and EC+CRC+other cancers.

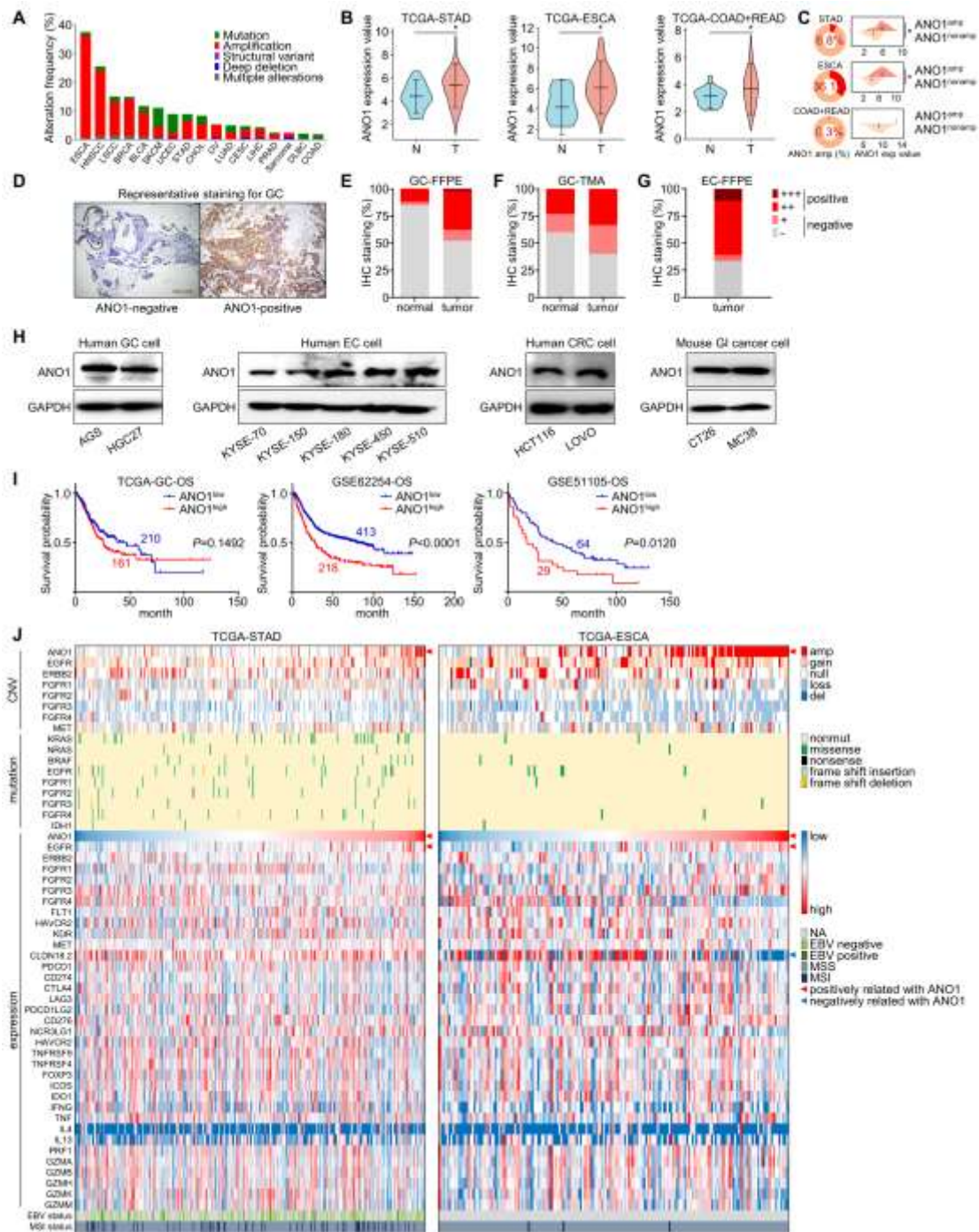


**Figure S2. The genetic and expressional landscape of ANO1 in GI cancers.**

(A) ANO1's genetic aberrance across TCGA cancer types. (B) Transcript levels of ANO1 in tumor (T) vs normal (N) tissues of TCGA-STAD/ESCA/COAD+READ datasets. (C) Transcript levels of ANO1 in ANO1 amplified vs nonamplified tumors of TCGA-STAD/ESCA/COAD+READ datasets. (D) Representative imaging of ANO1 IHC staining in GC tissues. Positivity rate of ANO1 in (E) a surgery GC cohort, (F) a tissue microarray (TMA) GC cohort and (G) an EC cohort. (H) ANO1 expression in multiple human and mouse GI cancer cells. (I) The prognostic correlation of ANO1 with OS in multiple GC datasets. (J) ANO1's distribution with major therapeutic biomarkers & targets of GI cancers in TCGA-STAD/ESCA datasets. \*,  $P < 0.05$ . Error bars, mean  $\pm$  SEM.

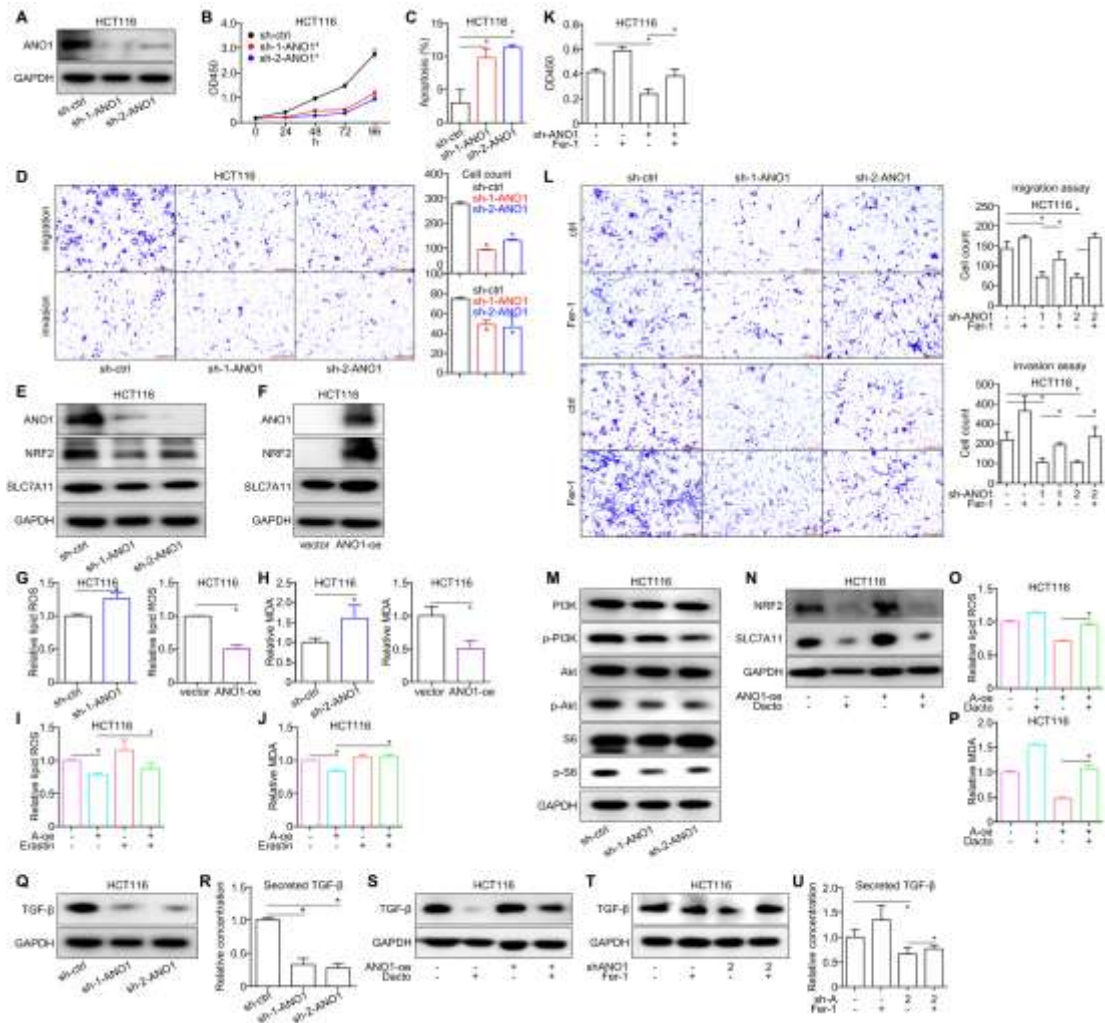


**Figure S3. The *in vitro* phenotypes & mechanisms of ANO1 were consistently observed for CRC cell.**

(A) ANO1 knockdown in CRC cell. Changes of *in vitro* (B) proliferation, (C) apoptosis and (D) invasiveness were measured after ANO1 knockdown. Expression of ferroptotic proteins after (E) ANO1 knockdown or (F) overexpression (oe) were assessed in CRC cell. The levels of (G) lipid ROS and (H) MDA after ANO1 knockdown or overexpression were assessed. (I) Lipid ROS and (J) MDA repressed by ANO1 overexpression was rescued by ferroptosis agonist Erastin in CRC cell. The *in vitro* (K) proliferation and (L) invasiveness suppressed by ANO1 knockdown were reversed by ferroptosis inhibitor Fer-1 in HCT116 cell. (M) ANO1 knockdown in CRC cell deactivated PI3K-Akt signaling. PI3K-Akt signaling inhibitor Dactolisib (Dacto) abrogated (N) the NRF2/SLC7A11 upregulation, rescued the (O) lipid ROS/(P) MDA inhibition. The (Q) expression and (R) secretion of TGF-β by CRC cell HCT116 were assessed after ANO1 knockdown. (S) PI3K-Akt signaling inhibitor Dactolisib (Dacto) repressed the TGF-β upregulation induced by ANO1 overexpression. The (T) expression and (U) secretion of TGF-β by CRC cell were reduced by ANO1 knockdown and rescued by ferroptosis inhibitor Fer-1. \*,  $P < 0.05$ . Error bars, mean  $\pm$  SEM.

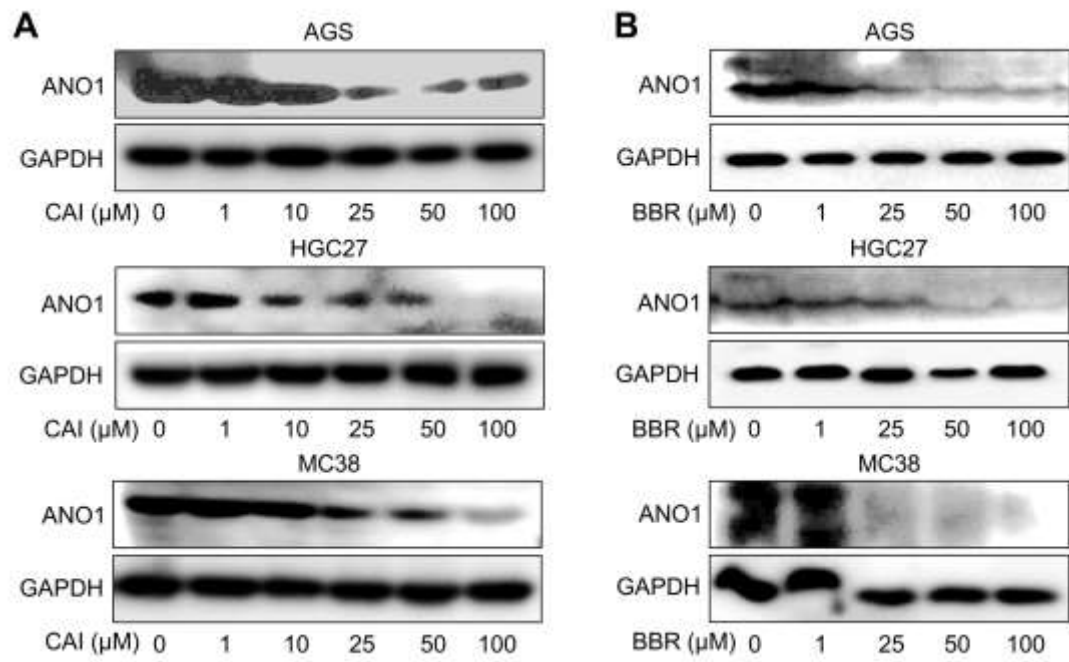


**Figure S4. ANO1 inhibitors repressed ANO1 expression in a dose-dependent manner.**

Changes of ANO1 protein expression in multiple GI cancer cells as the dose of ANO1 inhibitors (A) CaCCinh-A01 or (B) Benzbromarone escalating.

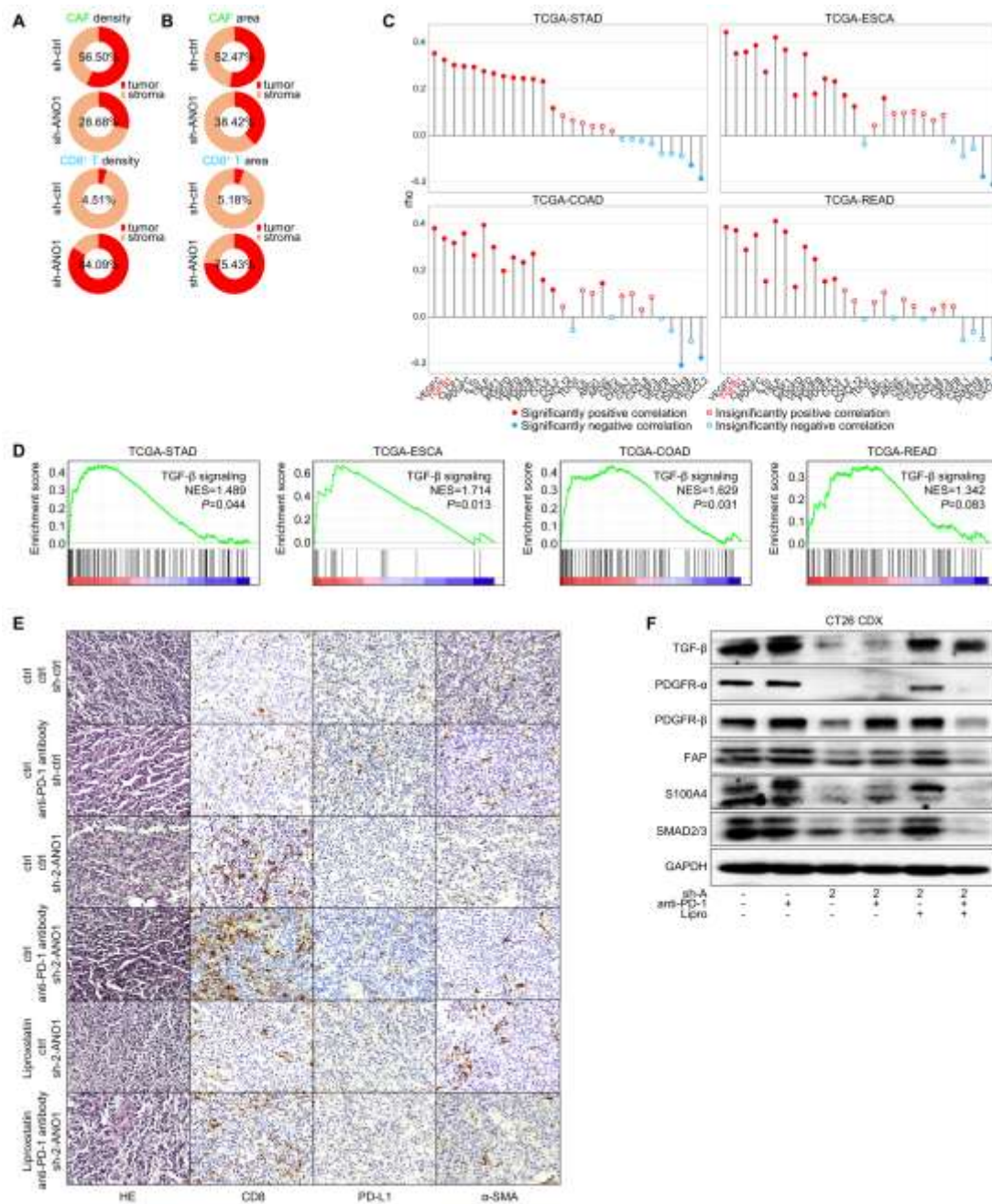


**Figure S5. ANO1 promotes CAF infiltration in TIME and facilitates the CAF secretome.**

The (A) density ratio and (B) area ratio of CAFs and CD8<sup>+</sup> T cells in tumor/stroma regions were assessed by mIHC analysis. (C) ANO1 expression displayed a high correlation with CAF secretome members across TCGA-STAD/ESCA/COAD/READ datasets. (D) ANO1-related enrichment of TGF- $\beta$  signaling in TCGA-STAD/ESCA/COAD/READ datasets. (E) IHC staining for infiltrated CD8/PD-L1/ $\alpha$ -SMA in CT26 xenograft tissue. (F) Immunoblot-based expression of TGF- $\beta$  and CAF markers in CT26 xenograft tissue.

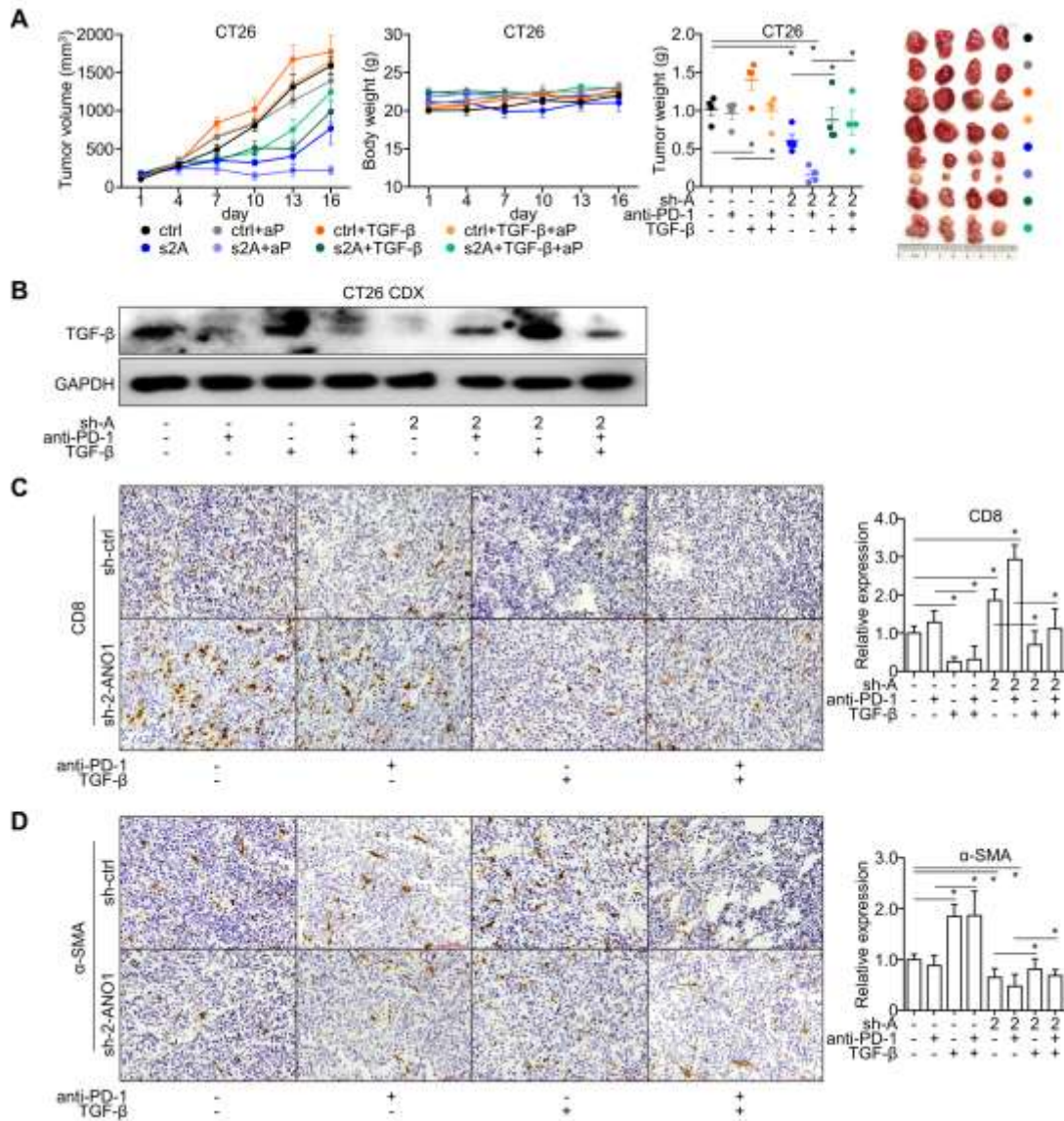


**Figure S6. The impact of ANO1-PI3K-Akt-ferroptosis axis on immunotherapy efficacy, CD8<sup>+</sup> T cell infiltration and CAF recruitment depends on TGF-β.**

(A) The sensitized anti-tumor effectiveness in CT26 CDX by combining ANO1 knockdown and anti-PD1 antibodies was alleviated by TGF-β. (B) The expression of TGF-β in CT26 CDX tissues were measured by immunoblot. CD8<sup>+</sup> T cell infiltration and CAF recruitment in CT26 CDX tissues were measured by staining (C) CD8 and (D) α-SMA with IHC. \*, *P*<0.05. Error bars, mean ± SEM.

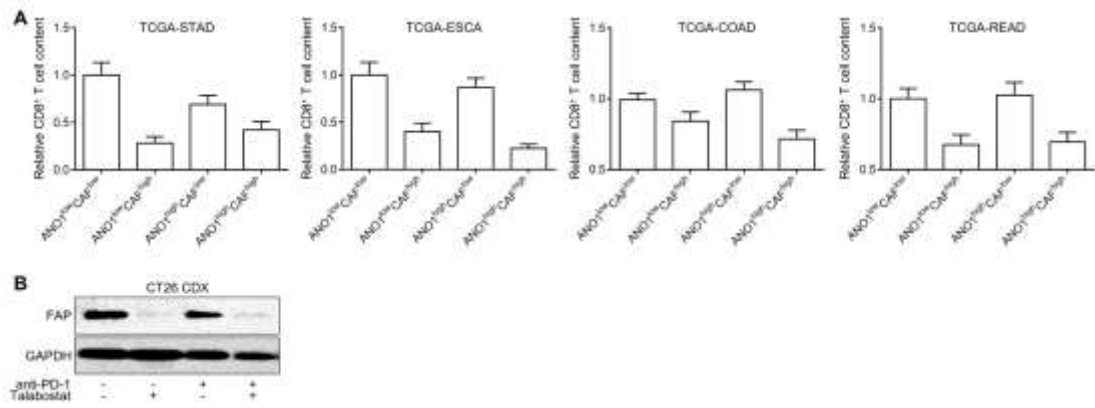
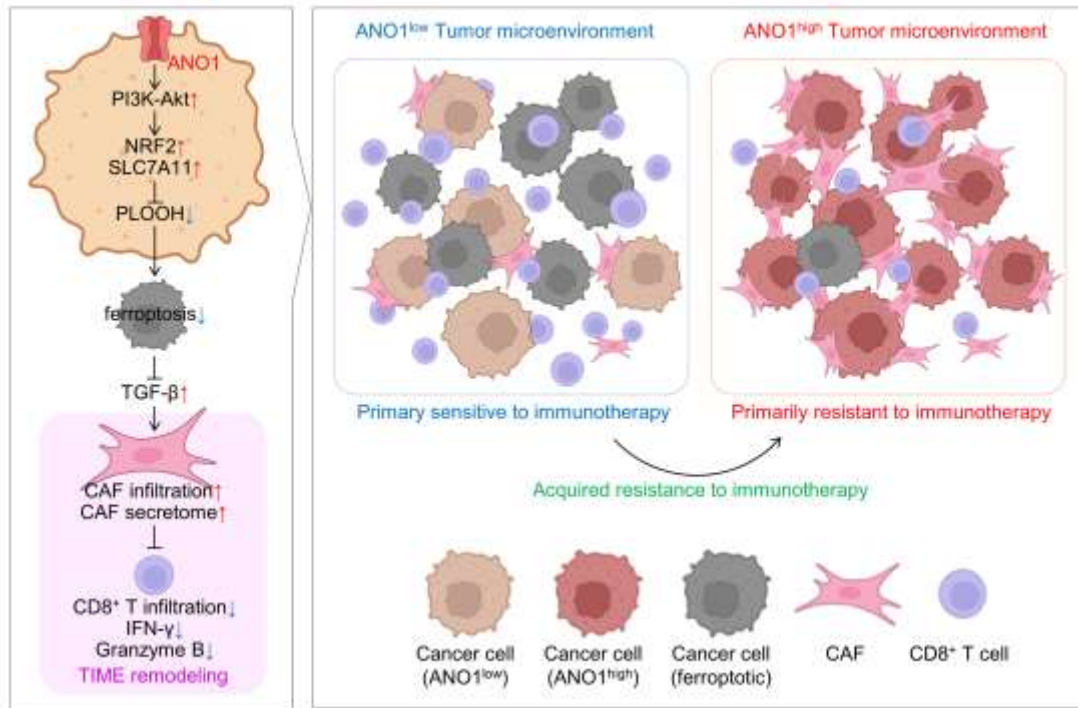


**Figure S7. The relationship among CD8<sup>+</sup> T cells, ANO1 and CAFs in GI cancers.**

(A) The content of CD8<sup>+</sup> T cells in TCGA-STAD/ESCA/COAD/READ datasets were stratified by ANO1 expression and CAF content. (B) The effect of Talabostat mesylate combined with anti-PD-1 antibodies on inhibiting FAP expression in CT26 CDX tissue. Error bars, mean ± SEM.



**Schematic chart**

**Table S1. Demographic features of the retrospective training cohort classified by ANO1 status.**

	99-case training cohort n (%)	ANO1 status (by DNA sequencing)		P value
		Non-amplification	Amplification	
Total		94	5	
Gender				0.673
	male	67 (71.3)	4 (80.0)	
	female	27 (28.7)	1 (20.0)	
Age				0.597
	≥60	49 (52.1)	2 (40.0)	
	<60	45 (47.9)	3 (60.0)	
Tumor type				0.054
	Esophageal cancer	23 (24.5)	4 (75.0)	
	Gastric cancer	36 (38.3)	1 (25.0)	
	Colorectal cancer	21 (22.3)	0 (0.0)	
	Others	14 (14.9)	0 (0.0)	
Stage				0.683
	I	0 (0.0)	0 (0.0)	
	II	0 (0.0)	0 (0.0)	
	III	3 (3.2)	0 (0.0)	
	IV	90 (95.7)	5 (100.0)	
	n/a	1 (1.1)	0 (0.0)	
HER2 positivity				1.000
	positive	4 (4.3)	0 (0.0)	
	negative	50 (53.2)	2 (40.0)	
	n/a	40 (42.6)	3 (60.0)	
CPS				0.245

	0	29 (30.9)	0 (0.0)	
	≥1	32 (34.0)	3 (60.0)	
	n/a	33 (35.1)	2 (40.0)	
MSI/MMR status				0.550
	MSI/dMMR	22 (23.4)	0 (0.0)	
	MSS/pMMR	49 (52.1)	3 (60.0)	
	n/a	23 (24.5)	2 (40.0)	
Regimen				0.422
	anti-PD-1/PD-L1	81 (86.2)	5 (100.0)	
	anti-PD-1/PD-L1 plus anti-CTLA4	9 (9.6)	0 (0.0)	
	anti-PD-1/PD-L1 plus chemotherapy	3 (3.2)	0 (0.0)	
	anti-PD-1/PD-L1 plus targeted therapy	1 (1.1)	0 (0.0)	
	anti-PD-1/PD-L1 plus chemotherapy plus targeted therapy	0 (0.0)	0 (0.0)	
Therapeutic line				0.525
	1	36 (38.3)	1 (20.0)	
	2	38 (40.4)	2 (40.0)	
	3 or higher	19 (20.2)	2 (40.0)	
	n/a	1 (1.1)	0 (0.0)	
Best response				0.102
	CR/PR	22 (23.4)	0 (0.0)	
	SD	24 (25.5)	0 (0.0)	
	PD	48 (51.1)	5 (100.0)	
	n/a	0 (0.0)	0 (0.0)	
	Median prognostic month			n/a
	irPFS	2.7 month	3.6 month	
	irOS	9.5 month	9.9 month	

**Table S2. Demographic features of the prospective validating cohort classified by ANO1 status.**

	48-case validating cohort n (%)	ANO1 status (by IHC)		P value
		Negative (-/+)	Positive (++/+++)	
Total		28	20	
Gender				0.537
	male	20 (71.4)	12(60.0)	
	female	8 (8.6)	8 (40.0)	
Age				0.394
	≥60	13 (46.4)	12 (60.0)	
	<60	15 (53.6)	8 (40.0)	
Tumor type				0.071
	Esophageal cancer	3 (10.7)	1 (5.0)	
	Gastric cancer	17 (60.7)	18 (90.0)	
	Colorectal cancer	8 (28.6)	1 (5.0)	
	Others	0 (0.0)	0 (0.0)	
Stage				1.0000
	I	0 (0.0)	0 (0.0)	
	II	0 (0.0)	0 (0.0)	
	III	1 (3.6)	0 (0.0)	
	IV	15 (53.6)	12 (60.0)	
	n/a	12 (42.9)	8 (40.0)	
HER2 positivity				0.744
	positive	6 (21.4)	7 (35.0)	
	negative	15 (53.6)	13 (65.0)	
	n/a	7 (25.0)	0 (0.0)	
CPS				0.680

	0	5 (17.9)	4 (20.0)	
	≥1	6 (21.4)	8 (40.0)	
	n/a	17 (60.7)	8 (40.0)	
MSI/MMR status				0.010
	MSI/dMMR	7 (25.0)	0 (0.0)	
	MSS/pMMR	16 (57.1)	20 (55.6)	
	n/a	5 (17.9)	0 (0.0)	
Regimen				0.765
	anti-PD-1/PD-L1	9 (32.1)	4 (20.0)	
	anti-PD-1/PD-L1 plus anti-CTLA4	3 (10.7)	1 (5.0)	
	anti-PD-1/PD-L1 plus chemotherapy	5 (17.9)	5 (25.0)	
	anti-PD-1/PD-L1 plus targeted therapy	8 (28.6)	8 (40.0)	
	anti-PD-1/PD-L1 plus chemotherapy plus targeted therapy	3 (10.7)	2 (10.0)	
Therapeutic line				0.722
	1	15 (53.6)	11 (55.0)	
	2	5 (17.9)	2 (10.0)	
	3 or higher	8 (28.6)	7 (35.0)	
Best response				0.392
	CR/PR	16 (57.1)	9 (45.0)	
	SD	9 (32.1)	7 (35.0)	
	PD	2 (7.1)	4 (20.0)	
	n/a	1 (3.6)	0 (0.0)	
Median prognostic month				n/a
	irPFS	14.9 month	5.7 month	
	irOS	Not reached	Not reached	

**Table S3. Univariate analysis for ANO1's correlation with immunotherapeutic outcomes in the training cohort.**

99-case training cohort	irPFS		irOS	
	Hazard ratio	<i>P</i> value	Hazard ratio	<i>P</i> value
Univariate analysis				
ANO1	2.884	0.025	2.424	0.143

**Table S4. Univariate analysis for ANO1's correlation with immunotherapeutic outcomes in the validating cohort.**

48-case validating cohort	irPFS		irOS	
	Hazard ratio	<i>P</i> value	Hazard ratio	<i>P</i> value
Univariate analysis				
ANO1	2.844	0.007	5.579	0.041